

advances.sciencemag.org/cgi/content/full/6/46/eabb2454/DC1

Supplementary Materials for

LRRK2 mediates tubulation and vesicle sorting from lysosomes

Luis Bonet-Ponce, Alexandra Beilina, Chad D. Williamson, Eric Lindberg, Jillian H. Kluss, Sara Saez-Atienzar, Natalie Landeck, Ravindran Kumaran, Adamantios Mamais, Christopher K. E. Bleck, Yan Li, Mark R. Cookson*

*Corresponding author: Email: cookson@mail.nih.gov

Published 11 November 2020, *Sci. Adv.* **6**, eabb2454 (2020)
DOI: 10.1126/sciadv.abb2454

The PDF file includes:

Figs. S1 to S7
Legends for movies S1 to S6
Legends for tables S1 to S3
Tables S4 and S5

Other Supplementary Material for this manuscript includes the following:

(available at advances.sciencemag.org/cgi/content/full/6/46/eabb2454/DC1)

Movies S1 to S6
Tables S1 to S3

SUPPLEMENTARY FIGURES:

Fig. S1

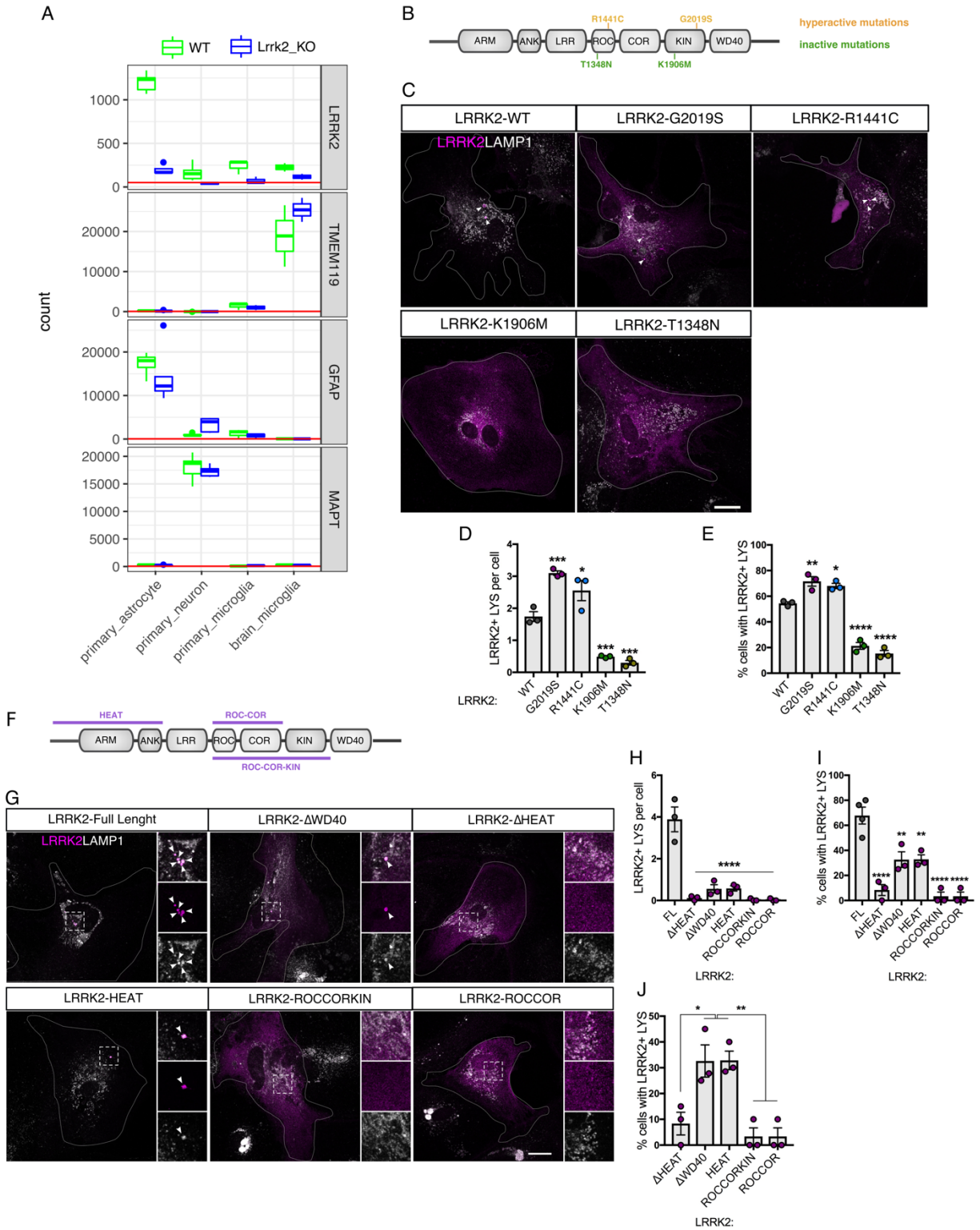


Fig. S2

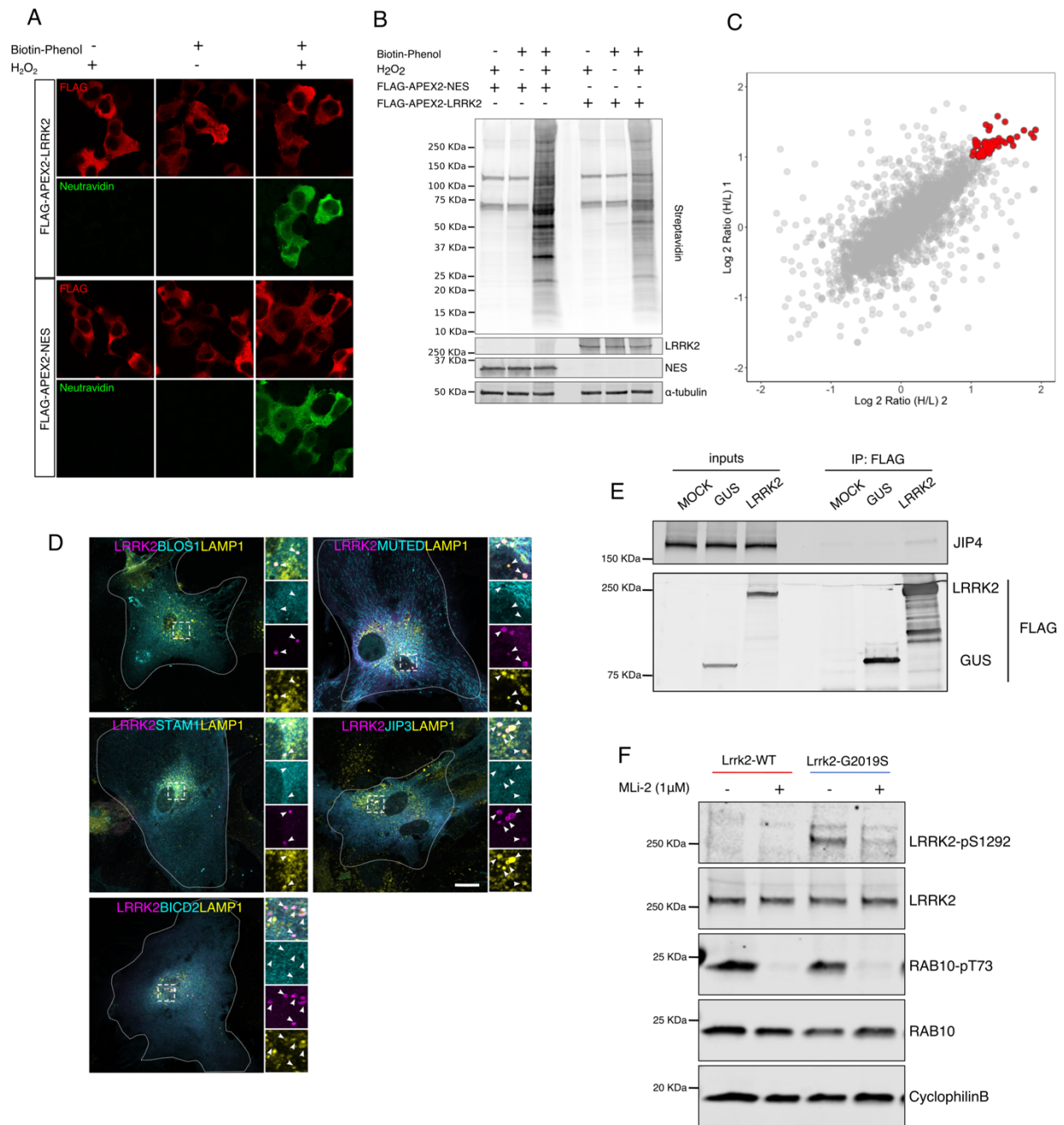


Fig. S3

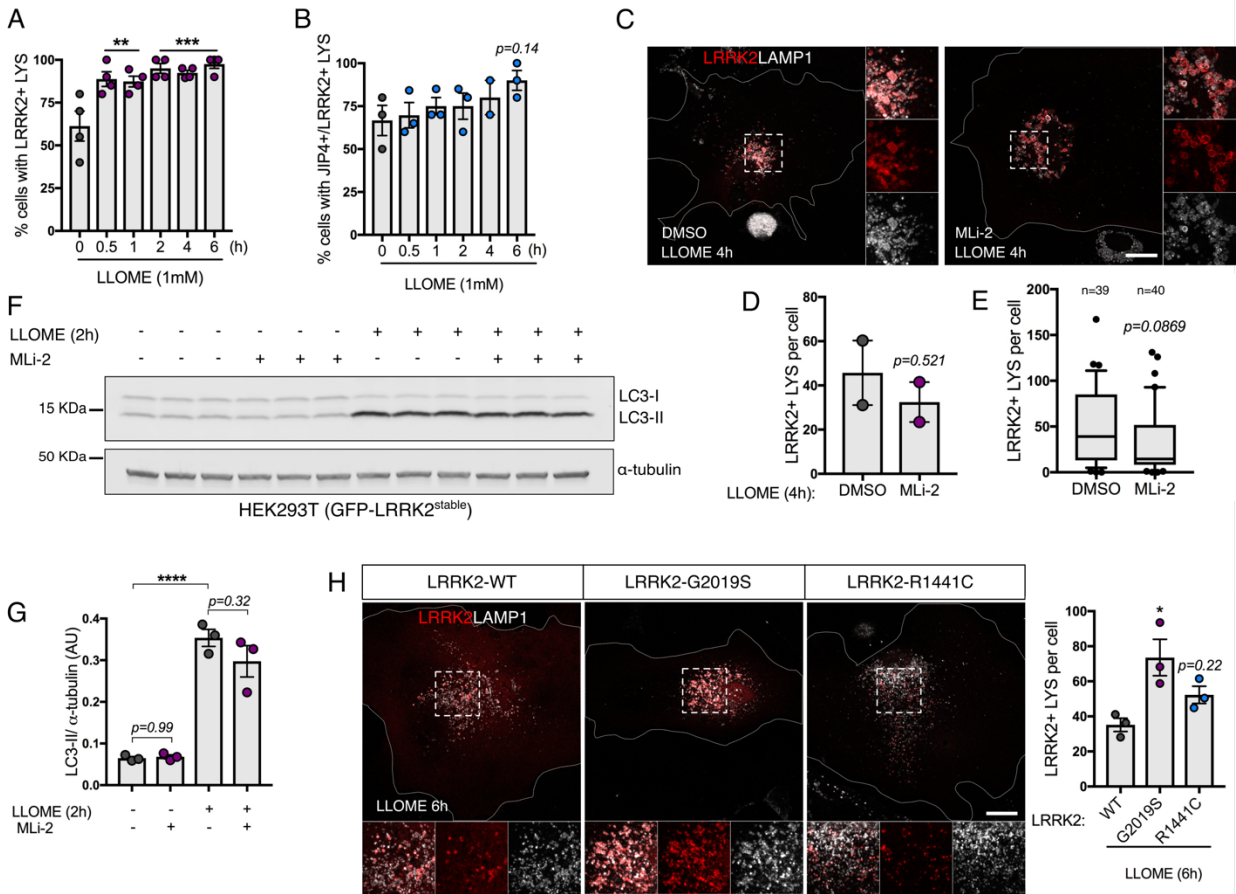
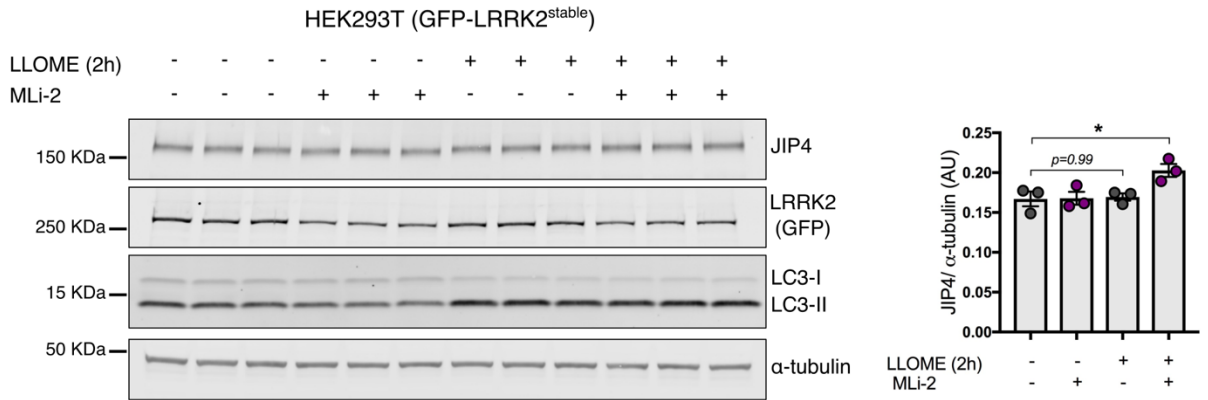
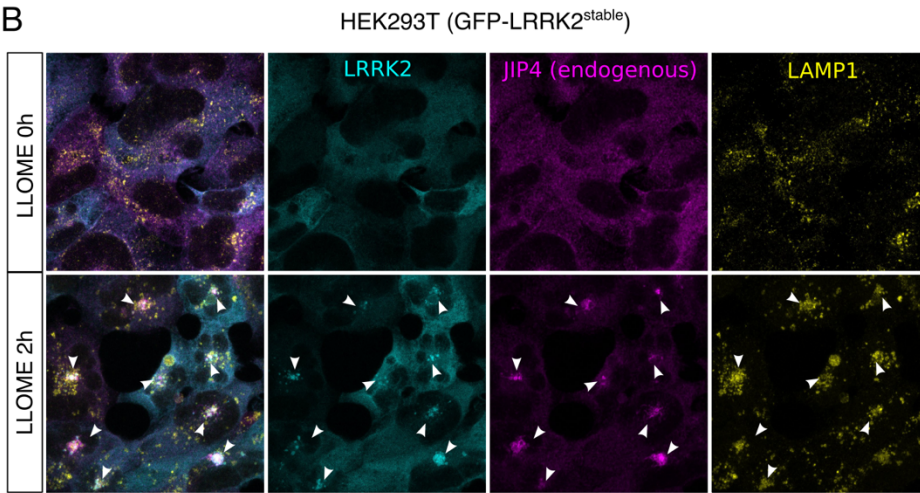


Fig. S4

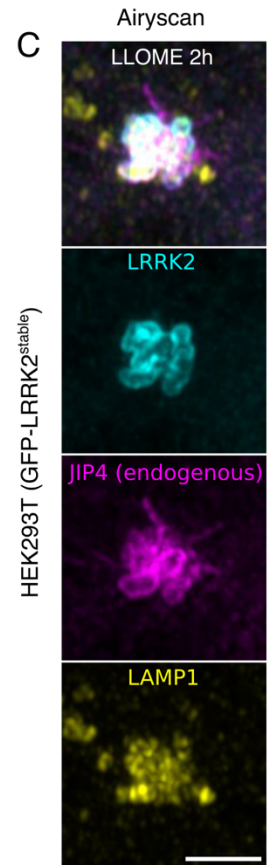
A



B



C



D

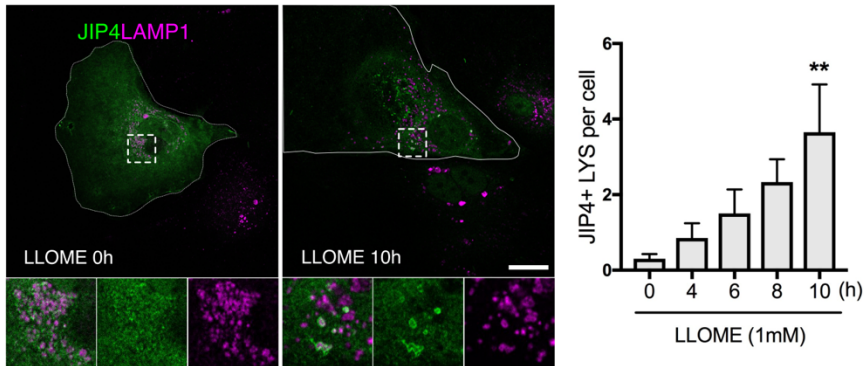


Fig. S5

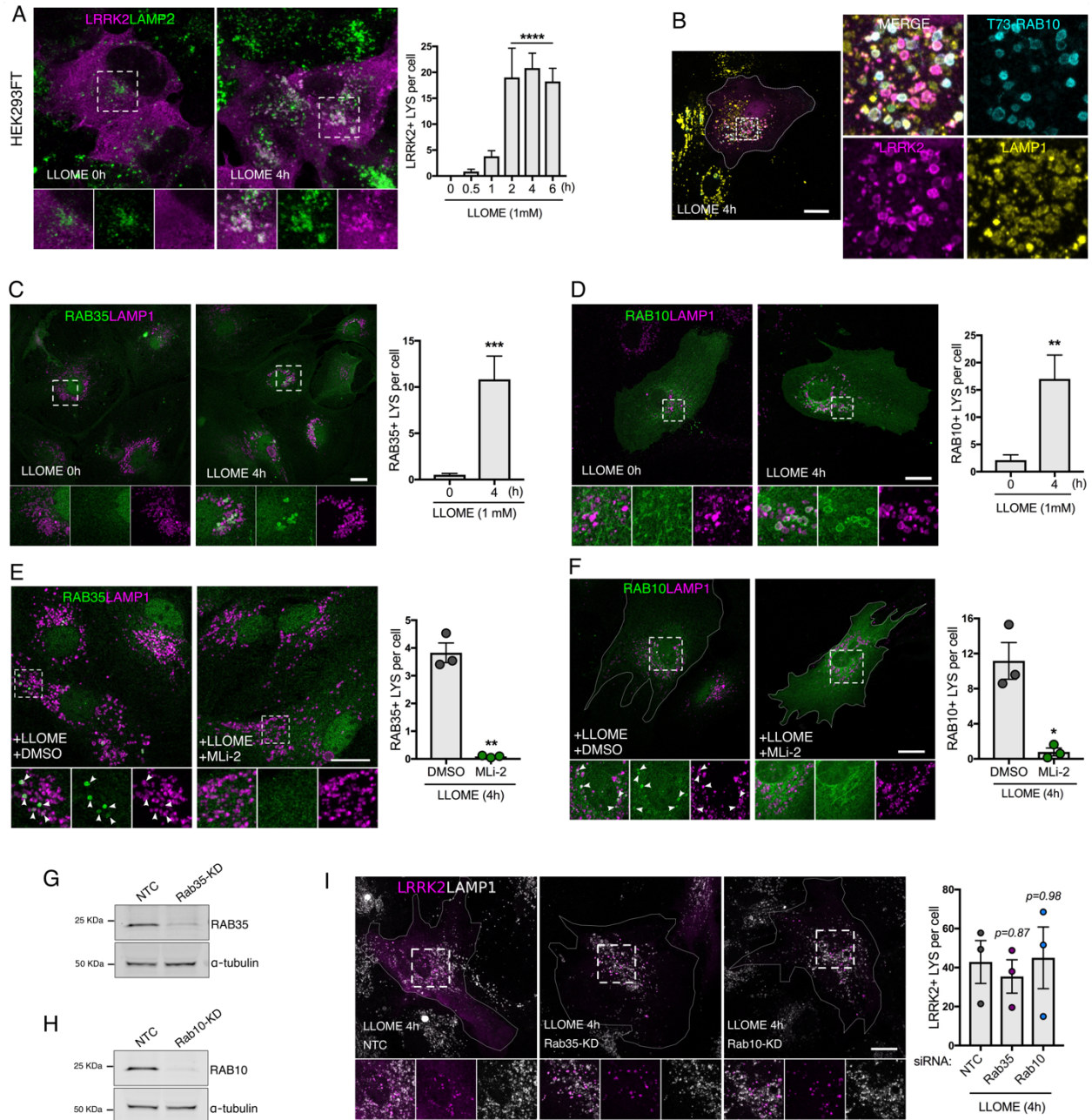


Fig. S6

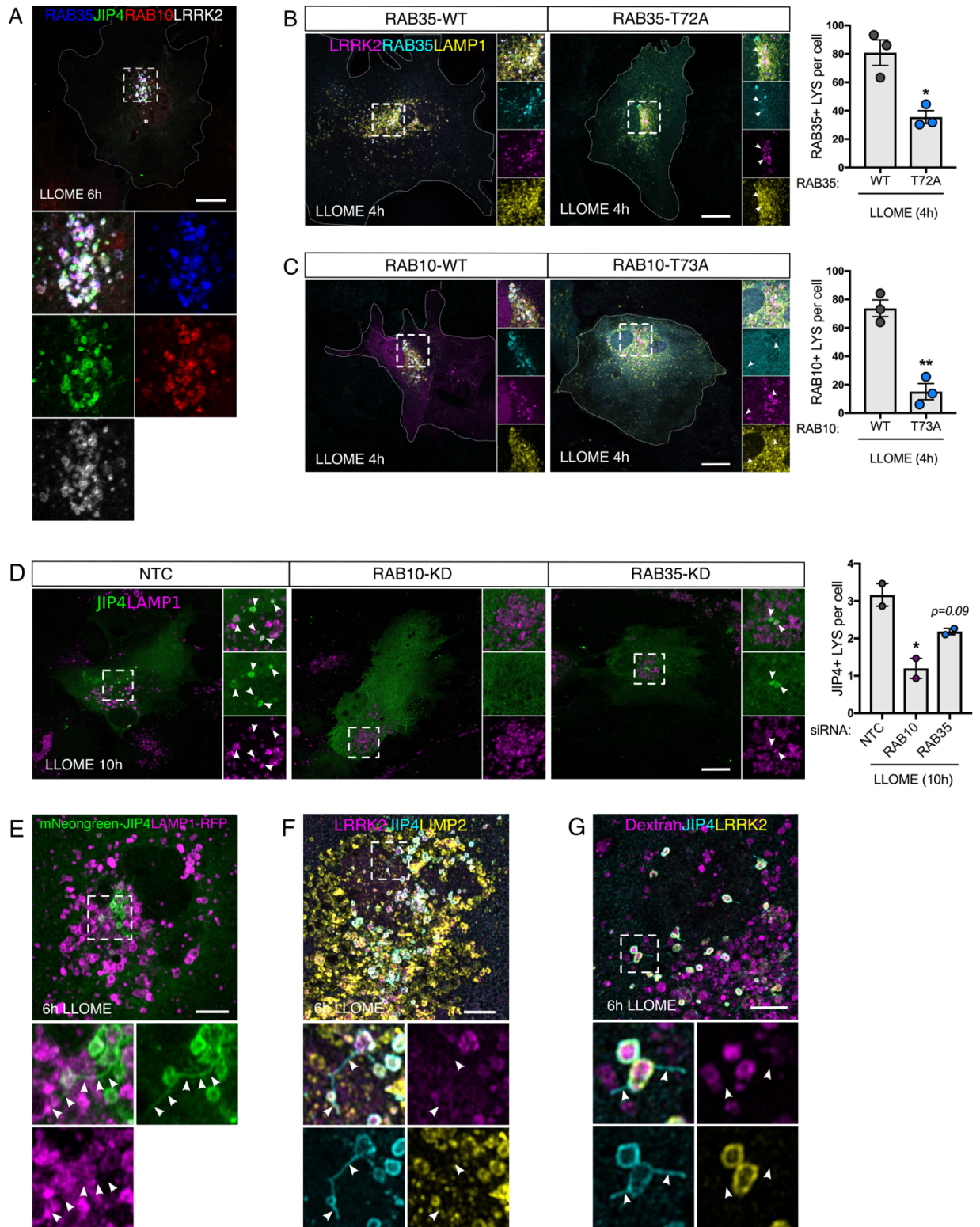
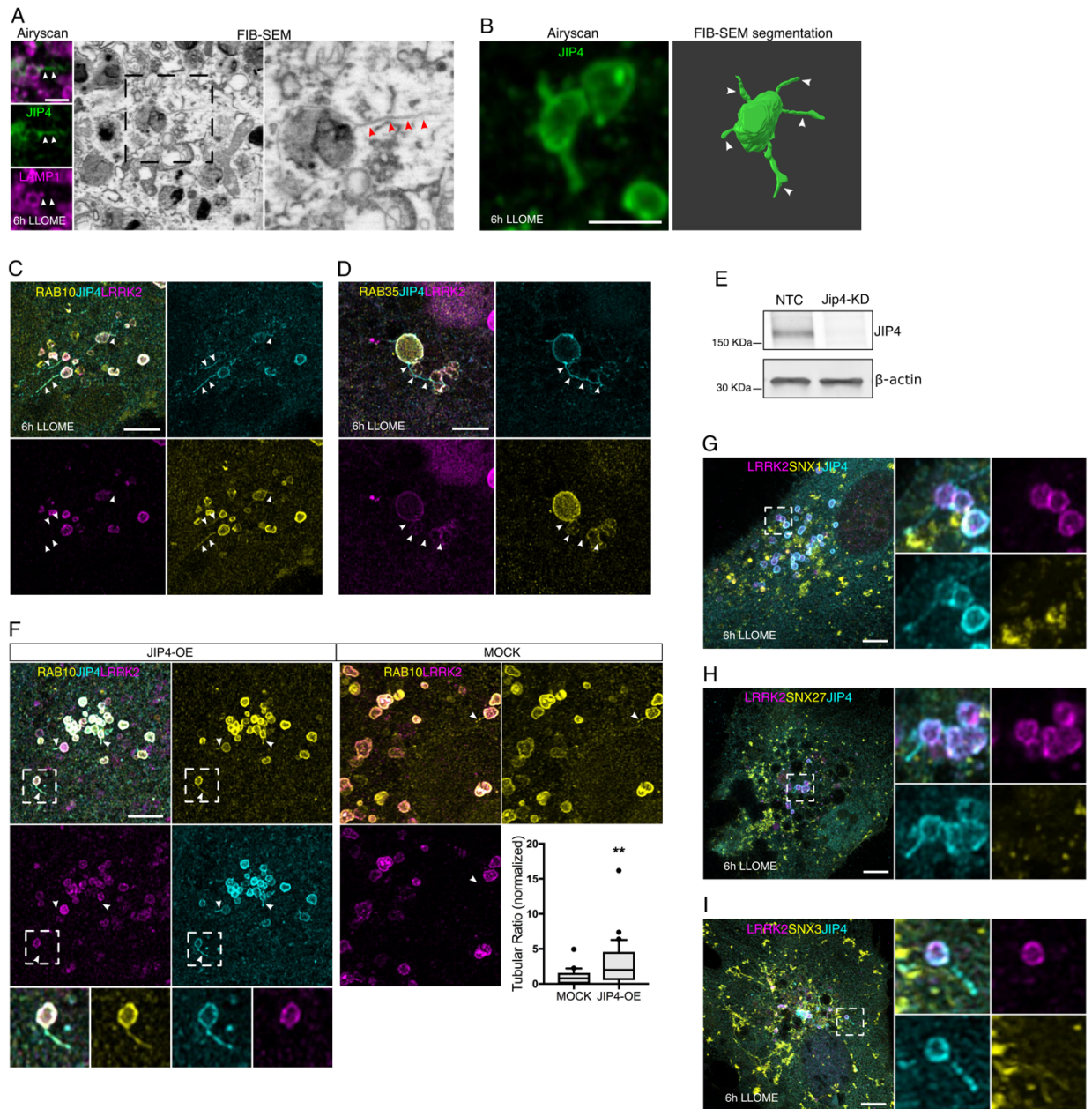


Fig. S7



SUPPLEMENTARY FIGURE LEGENDS:

SUPPLEMENTARY FIGURE S1. LRRK2 mutations and domain analysis affect the

lysosomal recruitment of LRRK2. **A.** Primary cultures of cortical astrocytes, cortical neurons and microglia were made from *Lrrk2*-WT and *Lrrk2*-KO mice and RNAseq was performed.

mRNA expression of GFAP (astrocyte marker), MAPT (neuron marker), TMEM119 (microglia marker) and LRRK2 was plotted comparing *Lrrk2*-WT and KO cells. **B.** Schematic

representation of LRRK2 and its domains, with pathogenic hyperactive mutations (R1441C and G2019S) in orange purple the artificial inactive mutations (T1348N and K1906M) in purple. **C.**

Representative confocal images of astrocytes expressing 3xflag-LRRK2-WT, 3xflag-LRRK2-G2019S, 3xflag-LRRK2-K1906M and 3xflag-LRRK2-T1348N and stained for LAMP1. The

number of LRRK2-positive lysosomes per cell (**D**) and the percentage of cells with lysosomal LRRK2 (**E**) were quantified and compared to the WT group in a one-way ANOVA with

Dunnett's *post-hoc* test ($n=20$ cells from $N=3$ independent experiments). Data are means \pm

SEM. Dots represent the mean of every independent experiment, N . **F.** Schematic representation of LRRK2 and its domains, marking the multi-domain plasmids used in this experiment in blue.

G. Representative confocal images of astrocytes transfected with 3xflag-LRRK2-Full Length, 3xflag-LRRK2- Δ HEAT, 3xflag-LRRK2- Δ WD40, 3xflag-LRRK2-HEAT, 3xflag-LRRK2-ROC-COR-KIN and 3xflag-LRRK2-ROC-COR and stained for LAMP1. **H-I.** The number of LRRK2-

positive lysosomes per cell (**H**) and the percentage of cells with lysosomal LRRK2 (**I**) were quantified comparing the full-length vector with all other constructs. Data are means \pm SEM.

Dots represent the mean of every N . One-way ANOVA with Dunnett's *post-hoc* test ($n=20$ cells per N from $N=3$). **J.** Histogram showing the percentage of cells with lysosomal LRRK2

comparing the domain constructs to each other. Data are means \pm SEM. Dots represent the mean of every N . One-way ANOVA was used with Tukey's *post-hoc* test ($n=20$ cells per N from $N=3$). White arrowheads indicate colocalization between LRRK2 and LAMP1. Scale bar: 20 μ m.

SUPPLEMENTARY FIGURE S2. Additional information on the APEX2 screening for

LRRK2-membrane partners. A. Representative confocal images of HEK293FT cells

expressing 3xflag-APEX2-LRRK2 and 3xflag-APEX2-NES and stained with Neutravidin to

detect biotinylation. **B.** Similar experiment where lysates were analyzed by western blot for

APEX2-tagged proteins. **C.** Full scatter plot of the two replicates of the APEX2-LRRK2

screening compared to APEX2-NES. Proteins that passed the threshold of 2-fold higher

abundance in the LRRK2 group compared to NES in both replicates are shown in red. **D.**

BLOS1, MUTED, JIP3, STAM1 and BICD2 were cloned in GFP constructs and expressed along

3xflag-LRRK2. No colocalization was observed between these proteins and LRRK2 in the

lysosomal membrane (white arrowheads). **E.** HEK293FT cells were either mock transfected or

transfected with 3xflag-tagged *E. coli* beta-glucuronidase (GUS) as negative controls or with

3xflag-LRRK2. Protein lysates were subjected to immunoprecipitation with anti-flag antibodies

and immunoblotted for endogenous JIP4 or FLAG, showing that LRRK2 interacts with JIP4. **F.**

Mouse primary astrocytes carrying the WT form or the G2019S mutation of LRRK2 were pre-

treated with DMSO or MLi-2, lysed and immunoblotted for LRRK2-pS1292, LRRK2, RAB10-

T73, RAB10 and cyclophilinB as a loading control. Scale bar: 20 μ m.

SUPPLEMENTARY FIGURE S3. Effect of MLi-2 and pathogenic hyperactive LRRK2

mutations in LRRK2 recruitment to lysosomes. A-B. Histogram showing the percentage of

cells with lysosomal LRRK2 (**A**) and lysosomal JIP4 (**B**) in cells treated or not with LLOME.

Data are means \pm SEM. Dots represent the mean of every N . One-way ANOVA with Dunnett's *post-hoc* test ($n=20$ cells per N from $N=3$). **C.** Representative confocal images of astrocytes expressing 3xflag-LRRK2 and LAMP1, pre-incubated with DMSO or MLI-2 and treated with LLOME. **D.** Histogram represents the number of LRRK2-positive lysosomes per cell. Data are means \pm SEM. Dots represent the mean of every N . Unpaired *t-test* was applied for $n=19-20$ from $N=2$ independent experiments. **E.** Box plot shows the median and the whiskers the 10-90th percentile, $n=39-40$ cells pooled from two experiments. **F.** DOX-inducible GFP-LRRK2 cells were pre-incubated with MLI-2 (90 min) before being treated or not with LLOME (1 mM, 2 h). Lysates were probed for LC3 and normalized by α -tubulin. **G.** Two-way ANOVA with Tukey's *post-hoc* ($n=3$). Error bars indicate SEM. **H.** Representative confocal images of astrocytes expressing 3xflag-LRRK2-WT, 3xflag-LRRK2-G2019S and 3xflag-LRRK2-R1441C and stained for LAMP1. The number of LRRK2-positive lysosomes per cell was measured using one-way ANOVA with Dunnett's *post hoc* test ($n=20$ cells per N from $N=3$). Data are means \pm SEM. Dots represent the mean of every N . Scale bar: 20 μ m.

SUPPLEMENTARY FIGURE S4. Additional information on JIP4 response to LLOME. A. DOX-inducible GFP-LRRK2 cells were pre-incubated with MLI-2 (90 min) before being treated or not with LLOME (1 mM, 2 h). Lysates were probed for JIP4 and LC3 (as a positive control for LLOME) and normalized by α -tubulin. Two-way ANOVA with Tukey's *post-hoc* ($n=3$). Data are means \pm SEM. **B.** Confocal images of DOX-inducible GFP-LRRK2 cells being treated or not with LLOME (1 mM, 2 h) and stained for endogenous JIP4 and LAMP1. White arrowheads indicate lysosomes positive for LRRK2 and JIP4. **C.** Airyscan images showing the presence of endogenous JIP4 in the lysosomal membrane in HEK293T cells 2 h after LLOME

addition. **D**. Representative confocal images of astrocytes expressing GFP-JIP4 and LAMP1, treated with LLOME. Histogram represents the number of JIP4-positive lysosomes per cell. Data are means \pm SEM. One-way ANOVA with Dunnett's *post hoc* test. Scale bar: 10 μ m (**B**), 3 μ m (**C**) and 20 μ m (**D**).

SUPPLEMENTARY FIGURE S5. Additional information on the link between LRRK2 and both RAB GTPases (RAB35 and RAB10) upon lysosomal membrane permeabilization. A.

Representative confocal images of HEK293FT cells expressing 3xflag-LRRK2 and LAMP2 and treated with LLOME. Histogram refers to the number of LRRK2-positive lysosomes per cell. Data are means \pm SEM. One-way ANOVA with Dunnett's test for multiple comparisons was applied, $n= 40-56$ cells per condition. **B**. Confocal image of a LLOME-treated cell (4 h) expressing 3xflag-LRRK2 and stained for endogenous LAMP1 and T73-RAB10. **C-D**.

Representative confocal images of astrocytes expressing RAB35 (**C**) or GFP-RAB10 (**D**) and LAMP1, treated or not with LLOME. Histogram depicts the number of RAB35-positive (**C**) or RAB10-positive (**D**) lysosomes per cell. Data are means \pm SEM. Unpaired *t-test* with Welch's correction was applied. **E-F**. Representative confocal images of astrocytes expressing RAB35 (**E**) or GFP-RAB10 (**F**) and LAMP1, pre-incubated with DMSO or MLI-2 in LLOME-treated cells. Histogram corresponds to the number of RAB35-positive (**E**) and RAB10-positive (**F**) lysosomes per cell. Data are means \pm SEM. Dots represent the mean of every N . Unpaired *t-test* with Welch's correction was applied, $n= 30-61$ cells (**E**), 19-20 cells (**F**) per N from $N= 3$. **G-H**. Astrocytes were exposed to NTC siRNA and Rab35 siRNA or Rab10 siRNA were lysed and immunoblotted for RAB35 (**G**) and RAB10 (**H**) and α -tubulin. **I**. Representative confocal images of astrocytes expressing 3xflag-LRRK2 and LAMP1 in cells knocked-down for Rab10 and

Rab35 and treated with LLOME (4 h), using an NTC as negative control. Histogram shows the number of LRRK2-positive lysosomes per cell. Data are means \pm SEM. Dots represent the mean of every N . One-way ANOVA with Dunnett's *post-hoc* test ($n=20$ per N from $N=3$). Scale bar: 20 μm .

SUPPLEMENTARY FIGURE S6. Additional information on RAB35/RAB10 and JIP4. A.

Confocal image shows an astrocyte expressing 2xmyc-RAB35, GFP-JIP4, RAB10 and 3xflag-LRRK2 in LLOME-treated cells. **B-C.** 3xflag-LRRK2 and LAMP1-HaloTag were transfected along 2xmyc-RAB35-WT or 2xmyc-RAB35-T72A (**B**), and 2xmyc-RAB10-WT or 2xmyc-RAB10-T73A (**C**) and treated with LLOME (4 h). The number of RAB35 or RAB10 lysosomal structures per cell was quantified ($n=12$ cells from three experiments). White arrowheads show colocalization. **D.** Astrocytes were incubated with NTC, RAB35 and RAB10 siRNA and 48 h later, transfected with GFP-JIP4 for an additional 48 h after. Cells were then treated with LLOME (10h) and the number of JIP4-positive LYS per cell was quantified. One-way ANOVA with Dunnett's *post-hoc* ($n=30$ cells per N , with $N=2$). Error bars indicate range. **E.** Airyscan live cell super-resolution image of an astrocyte expressing 3xflag-LRRK2-G2019S, mNeonGreen-JIP4 and LAMP1-RFP (LLOME, 6 h). **F.** Super-resolution image of an astrocyte expressing 3xflag-LRRK2-G2019S, GFP-JIP4 and LIMP2-myc (LLOME, 6 h). **G.** LLOME-treated (6 h) astrocyte expressing 3xflag-LRRK2-G2019S and GFP-JIP4 and incubated with Dextran-555. White arrowheads indicate JIP4-positive lysosomal tubules. Scale bar= 20 μm (**A-D**), 5 μm (**E-G**).

SUPPLEMENTARY FIGURE S7. Additional characterization of JIP4-positive tubular structures.

A. Representative FIB-SEM image of a thin JIP4-positive tubule in a 3xflag-

LRRK2-G2019S transfected astrocyte treated with LLOME (6 h). Upper panel shows the airyscan image of a JIP4-positive lysosome forming a thin tubule (white arrowhead). Lower panel shows the correlated EM image with a red arrowhead pointing to the lysosomal tubule. **B**. An example of the morphological diversity of the JIP4-positive tubules revealed by FIB-SEM. Left picture shows the airyscan image of a JIP4-positive lysosome forming five different tubules. Left picture shows the segmented 3D reconstruction from the correlated electron microscopy image with white arrowheads marking the different tubules (LLOME, 6 h). **C-D**. Astrocytes exogenously expressing 3xflag-LRRK2-G2019S and GFP-JIP4 and exposed to LLOME (6 h), were stained for endogenous RAB10 (**C**) and endogenous RAB35 (**D**). **E**. Astrocytes were treated with NTC or Jip4 siRNA. Western Blot shows JIP4 expression. **F**. Confocal super-resolution images of astrocytes expressing 3xflag-LRRK2-G2019S, RAB10 and MOCK or GFP-JIP4 transfected. LLOME was added for 6 h. RAB10 tubulation index was measured using an unpaired *t-test* with Welch's correction ($n=30$ cells pooled from two independent experiments). Box plot shows the median and the whiskers the 10-90th percentile. **G-I**. Airyscan images of LLOME-treated astrocytes (6 h) expressing 3xflag-LRRK2-G2019S, 2xmyc-JIP4 and (**G**) GFP-SNX1, (**H**) GFP-SNX27, (**I**) GFP-SNX3. White arrowheads indicate JIP4-positive lysosomal tubules. Scale bar= 2 μm (**B**), 5 μm .

SUPPLEMENTARY MOVIE 1. JIP4-positive tubules are negative for LRRK2 and LAMP1. Astrocytes expressing 3xflag-LRRK2, GFP-JIP and stained for LAMP1 were treated with LLOME for 6 h. Super-resolution stack was taken using airyscan and 3D reconstruction was made using Imaris software. Video was acquired at 15 frames/ second.

SUPPLEMENTARY MOVIE 2. FIB-SEM reveals the morphological heterogeneity of the JIP4-positive tubules. FIB-SEM segmentation of a JIP4-positive lysosome (from Figure S5D), in astrocytes treated with LLOME (6h), forming five tubules with different size and thickness. Segmentation was performed with Amira software.

SUPPLEMENTARY MOVIE 3. Super-resolution live cell imaging on JIP4-positive tubules. Confocal microscopy of JIP4-positive tubules budding, extending and releasing vesicular structures in a living astrocyte expressing 3xflag-LRRK2-G2019S and mNeonGreen-JIP4 (green) treated with LLOME for 6 h. Video was acquired at 1 second/ frame for 20 and 18 seconds, and played at a speed of 3 frames/ second). Video corresponds to Figure 7A. White arrowheads indicate JIP4-positive lysosomal tubules, yellow arrowheads show resolved tubules (vesicular structures and scissioned tubules).

SUPPLEMENTARY MOVIE 4. Released vesicular structure interacting with other lysosomes. Confocal microscopy of JIP4-release vesicular structure contacting with lysosomes, in a living astrocyte expressing 3xflag-LRRK2-G2019S, LAMP1-HaloTag (magenta) and mNeonGreen-JIP4 (green) treated with LLOME for 6 h. Video was acquired at 1 second/ frame for 34 seconds and played at a speed of 3 frames/ second). Video corresponds to Figure 7C. White arrowheads indicate JIP4-positive lysosomal tubules, yellow arrowheads show resolved tubule (vesicular structure).

SUPPLEMENTARY MOVIE 5. Moving vesicle temporary interacting with a lysosome. Confocal microscopy from the same cell as Figure 7C and Suppl movie 2. 3xflag-LRRK2-G2019S, mNeonGreen-JIP4 (green) and LAMP1-HaloTag (magenta) were transfected in primary astrocytes and treated with LLOME for 6 h. Video was acquired at 1 second/ frame for

56 seconds and played at a speed of 6 frames/ second. White arrowheads show moving JIP4-positive vesicle.

SUPPLEMENTARY MOVIE 6. Super-resolution live cell imaging on vesicle contacting an active lysosome. Confocal microscopy of JIP4-release vesicular structure contacting an active lysosome, in a living astrocyte expressing 3xflag-LRRK2-G2019S, and mNeonGreen-JIP4 (green) treated with LLOME for 6 h and incubated with MagicRed-CathepsinB (red) for 30 min. Each frame was acquired after 6.05 seconds, for 230 seconds (and played at a speed of 8 frames/ second). White arrowheads indicate JIP4-positive vesicular structure interacting with a MR-CTSB-positive lysosome.

SUPPLEMENTARY TABLES:

Table S1. LRRK2 vs NES proximity ligation screening

Table S2. List of 64 LRRK2 potential interactors

Table S3. LRRK2-APEX2 screening in the presence of LLOME

Table S4. List of expression vectors used in this study

PLASMID	STUDY
3xflag-LRRK2-WT	<i>Greggio et al., 2008</i>
3xflag-LRRK2-G2019S	<i>Beilina et al., 2014</i>
3xflag-LRRK2-R1441C	<i>Beilina et al., 2015</i>
3xflag-LRRK2-K1906M	<i>Beilina et al., 2016</i>
3xflag-LRRK2-T1348N	<i>Beilina et al., 2017</i>
3xflag-LRRK2-HEAT	<i>Greggio et al., 2008</i>
3xflag-LRRK2-ΔHEAT	<i>Greggio et al., 2009</i>
3xflag-LRRK2-ΔWD40	<i>Greggio et al., 2010</i>
3xflag-LRRK2-ROCCORKIN	<i>Greggio et al., 2011</i>
3xflag-LRRK2-ROCOR	<i>Greggio et al., 2012</i>
3xflag-APEX2-LRRK2	<i>This study</i>
3xflag-APEX2-NES	<i>This study</i>
GFP-JIP4	<i>This study</i>
mNeonGreen-JIP4	<i>This study</i>
GFP-JIP3	<i>This study</i>
GFP-STAM1	<i>This study</i>
GFP-BLOS1	<i>This study</i>
GFP-MUTED	<i>This study</i>
GFP-BICD2	<i>This study</i>
EmGFP-LRRK2	<i>This study</i>
EGFP-RAB10	<i>Gift from Marci Scidmore</i>
GFP-RAB35	<i>This study</i>
2xmyc-RAB10	<i>This study</i>
2xmyc-RAB35	<i>This study</i>
2xmyc-RAB10-T73A	<i>This study</i>
2xmyc-RAB35-T72A	<i>This study</i>
EGFP-GAL3	<i>Gift from Tamotsu Yoshimori</i>
LAMP1-RFP	<i>Gift from Walther Mothes</i>
LAMP1-HaloTag	<i>From Bonifacino lab</i>
LIMP2-myc	<i>Gift from Micahel Schwake</i>

Table S5. List of primers used for cloning

Primer name	Sequence
BLOS1_FOR	ctgtccgcctcctaaaagaaca
BLOS1_REV	ctaggaaggggcagactgca
MUTED_FOR	agtggcggaggacaga
MUTED_REV	ttaaaggttgaaaattcgctagtcctt
STAM1_FOR	cctcttttgccaccaatc
STAM1_REV	ctaggaaggctgggtt
JIP4_FOR	ATGGAGCTGGAGGACGGTGT
JIP4_REV	TCACTCATTGCCATACATCACTTGCCACACTA
RAB35_REV	ttagcagcagcgtttctttcgtttac
RAB35_FOR	ATGGCCCGGGACTACGA
RAB10_FOR	atggcgaagaagacgtacgacct
RAB10_REV	TCAGCAGCATTTGCTCTTCCA
RAB35_T72A_FO R	gtggaggtgatggcgcggaagcgctcc
RAB35_T72A_REV	ggagcgcttccgcgcatcacctccac
RAB10_T73A_FO R	taggaggttgatggcgtgaaatcgctcctgg
RAB10_T73A_REV	ccaggagcgatttcacgcatcacaacctccta